Integration and propagation of somatosensory responses in the corticostriatal pathway: an intracellular study *in vivo*

Morgane Pidoux[1], Séverine Mahon[1], Jean-Michel Deniau[2,3] and Stéphane Charpier[1,3]

[1] *Centre de Recherche de l'Institut du Cerveau et de la Moelle épinière, UPMC/INSERM UMR-S 975; CNRS UMR 7225, Hôpital Pitié-Salpêtrière, F-75013, Paris, France*
[2] *Institut National de la Santé et de la Recherche Médicale U667, Collège de France, F-75231 Paris cedex 05, France*
[3] *UPMC Univ Paris 06, F-75005, Paris, France*

Non-technical summary The striatum is a deep-brain region that controls sensory-guided behaviours. It is proposed that this striatal function is achieved by the integration of sensory information arising from the cerebral cortex. By means of *in vivo* electrophysiological tools, we examine in the rat how natural sensory events are integrated in cortical neurons and subsequently processed in their neuronal targets in the striatum. Although cortical neurons are reliably excited by the sensory stimulus, we found that neurons in the striatum display either no sensory response or a synaptic excitation that is able to produce a functional signal in only half of the neurons. These data show that the propagation of the sensory flow from the cortex to the striatum results in a refinement of external information that could allow the selection of more appropriate behaviours.

Abstract The dorsolateral striatum is critically involved in the execution and learning of sensorimotor tasks. It is proposed that this striatal function is achieved by the integration of convergent somatosensory and motor corticostriatal (CS) inputs in striatal medium-spiny neurons (MSNs). However, the cellular mechanisms of integration and propagation of somatosensory information in the CS pathway remain unknown. Here, by means of *in vivo* intracellular recordings in the rat, we analysed how sensory events generated by multi-whisker deflection, which provide essential somaesthetic information in rodents, are processed in contralateral barrel cortex layer 5 neurons and in the related somatosensory striatal MSNs. Pyramidal layer 5 barrel cortex neurons, including neurons antidromically identified as CS, responded to whisker deflection by depolarizing postsynaptic potentials that could reliably generate action potential discharge. In contrast, only half of recorded somatosensory striatal MSNs displayed whisker-evoked synaptic depolarizations that were effective in eliciting action potentials in one-third of responding neurons. The remaining population of MSNs did not exhibit any detectable electrical events in response to whisker stimulation. The relative inconstancy of sensory-evoked responses in MSNs was due, at least in part, to a Cl^--dependent membrane conductance concomitant with the cortical inputs, which was probably caused by whisker-induced activation of striatal GABAergic interneurons. Our results suggest that the propagation of whisker-mediated sensory flow through the CS pathway results in a refinement of sensory information in the striatum, which might allow the selection of specific sets of MSNs that are functionally significant during a given somaesthetic-guided behaviour.

(Received 19 September 2010; accepted after revision 5 November 2010; first published online 8 November 2010)
Corresponding author S. Charpier: Centre de Recherche de l'Institut du Cerveau et de la Moelle épinière, UPMC/INSERM UMR-S 975; CNRS UMR 7225, Hôpital Pitié-Salpêtrière, 91 Boulevard de l'hôpital, F-75013, Paris, France. Email: stephane.charpier@upmc.fr

Abbreviations CS, corticostriatal; dPSPs, depolarizing postsynaptic potentials; ECoG, electro-corticographic; ERPs, event-related potentials; KAc, potassium acetate; MSNs, medium-sized spiny neurons; PHA-L, *Phaseolus vulgaris* leucoagglutinin; *V*–*I*, voltage–current.

DOI: 10.1113/jphysiol.2010.199646

Introduction

The dorsolateral striatum integrates sensorimotor information that is encoded by patterned corticostriatal (CS) inputs arising from motor and somatosensory cortical areas (Flaherty & Graybiel, 1994, 1995; Deniau *et al.* 1996; Alloway *et al.* 2006), a process suggested to be involved in regulation, correct sequencing and learning of voluntary behaviour tasks (Graybiel *et al.* 1994; Barnes *et al.* 2005; Graybiel, 2008; Pennartz *et al.* 2009). In rodents, the whisker-related somatosensory system allows a tactile-mediated internal representation of the proximal environment, sensory information that guides exploratory behaviours in progress and participates in the planning of future action (Brecht, 2007; Petersen, 2007). The elucidation of integration processes of whisker-generated sensory responses in the related CS pathway is thus of crucial importance for establishing a cellular basis of striatum-related somaesthetic-guided behaviours.

Sensory events generated by whisker deflection access the dorsolateral striatum via a polysynaptic pathway sequentially composed of primary sensory neurons connecting, by glutamatergic synapses, trigeminal nuclei neurons. The latter convey sensory information to contralateral ventral posteromedial and medial posterior thalamic nuclei, where a second glutamatergic synapse excites thalamocortical neurons projecting to the primary somatosensory barrel cortex (Petersen, 2007). Thalamocortical axons originating from the ventral posteromedial nucleus form discrete clusters in layer 4 that provide the basis of the 'barrel' map. Barrel cortex neurons projecting bilaterally to the striatum are distributed uniformly across layer 5 and aligned with barrel or septal compartments (Wright *et al.* 2001; Alloway *et al.* 2006) with a significantly higher number of ipsilateral projections (Alloway *et al.* 2006). Corticostriatal projections from the whisker barrel cortex have a crude somatotopic organization and terminate in densely packed clusters with distributed bead varicosities that occupy curved lamellar-shaped regions along the dorsolateral edge of the neostriatum (Alloway *et al.* 1999).

Although it has been shown that neurons of the dorsolateral striatum could fire in response to cutaneous, visual and auditory stimuli (Wilson *et al.* 1983; Strecker *et al.* 1985; Carelli & West, 1991), little information is available about the cellular and synaptic integrative properties of the whisker-sensitive CS system. However, consistent with the CS projections from the barrel cortex, mechanical stimulation of vibrissae increases both glucose utilization (Brown *et al.* 1996, 2002) and the firing rate of extracellularly recorded single units (Carelli & West, 1991) in the contralateral dorsolateral striatum. Moreover, electrical stimulation of the whisker pad induces synaptic depolarizations in neurons located in the somatosensory striatum (Wright *et al.* 2001).

Here, we investigated, for the first time at the intracellular level, how sensory events generated by multiple-whisker deflection are processed in the CS pathway. Using *in vivo* intracellular recordings in the rat, we first examined the sensory-evoked responses in layer 5 barrel cortex pyramidal cells, including neurons antidromically identified as CS. Medium-sized spiny neurons (MSNs), known to integrate and convert cortical inputs into functionally relevant striatal outputs (Wilson, 1995*a*; Stern *et al.* 1997; Mahon *et al.* 2001, 2004), were then intracellularly recorded in the striatal sector receiving barrel cortex inputs and their sensory responses were analysed and compared to those recorded in CS cells. Whereas CS neurons showed a highly reliable synaptic activation following whisker deflection, the corresponding MSNs could be subcategorized as a function of their responsiveness to sensory inputs, including neurons without detectable response, neurons displaying subthreshold synaptic depolarizations, and cells that could be depolarized above spike threshold.

Methods

Ethical approval

All surgical and experimental procedures were in accordance with European Union (directive 86/609/EEC) and INSERM guidelines and complied with *The Journal of Physiology*'s policies on animal experimentation (Drummond, 2009). Every precaution was taken to minimize stress and the number of animals used in each series of experiments.

Animal preparation

Experiments were performed *in vivo* using 77 adult male Sprague–Dawley rats (8–15 weeks old) (Charles River, L'Arbresle, France). Animals were initially anaesthetized with sodium pentobarbital (40 mg kg^{-1}, I.P.; CEVA Santé Animale, Libourne, France) and ketamine (100 mg kg^{-1}, I.M.; Imalgène, Merial, France). A cannula was inserted into the trachea and the animal was placed in a stereotaxic frame. Wounds and pressure points were repeatedly (every 2 h) infiltrated with lidocaine (lignocaine, 2%). Once the surgical procedures had been completed, additional doses of pentobarbital (10–15 mg kg^{-1}, I.P.) were regularly administered and the depth of anaesthesia was assessed by continuous monitoring of heart rate and surface electro-corticographic (ECoG) activity. In a restricted number of experiments ($n = 13$ adult male Sprague–Dawley rats), analgesia was achieved, and rats maintained in a narcotized and sedated state,

by injections of fentanyl (3 μg kg^{-1}, I.P.; Janssen-Cilag, Issy-les-Moulinaux, France) repeated every 20–30 min (Mahon *et al.* 2001; Polack & Charpier, 2006). To obtain long-lasting stable intracellular recordings, rats were then immobilized with gallamine triethiodide (40 mg, I.M., every 2 h; Sigma, France) and artificially ventilated. Body temperature was maintained (36.5–37.5°C) with a homeothermic blanket. At the end of the experiments, animals received an overdose of sodium pentobarbital (200 mg kg^{-1}, I.P.).

Electrophysiological recordings

Spontaneous ECoG activity and surface event-related potentials (ERPs) (Fig. 1*A* and *B*), evoked by contralateral stimulations of whiskers (see below), were recorded with a low impedance (~60 kΩ) silver electrode placed on the dura above the primary somatosensory barrel cortex (6.8–7.3 mm anterior to the interaural line; 5 mm lateral to the midline) (Paxinos & Watson, 1986). The reference electrode was placed in a muscle on the opposite side of the head.

Intracellular recordings were performed using glass micropipettes filled with 2 M potassium acetate (KAc; 50–80 MΩ). In one experimental series (see Fig. 7*A–C*), MSNs were intracellularly recorded with KCl-filled microelectrodes (3 M, 30–40 MΩ). For intracellular labelling, 1% Neurobiotin (Vector Laboratories, Burlingame, CA, USA) was added to the micropipette solution. Single-unit extracellular recordings and juxtacellular labelling (see below) of striatal cells were made with glass electrodes (7–15 MΩ) filled with 0.5 M NaCl and 1.7% Neurobiotin.

The value of membrane potential was calculated as the mean of the distribution of spontaneous subthreshold activity (10 s duration). The membrane potential values were eventually corrected when a tip potential was recorded after termination of the intracellular recording. Measurements of apparent membrane input resistance and time constant were based on the linear electrical cable theory applied to an idealized isopotential neuron (Rall, 1969). Apparent membrane input resistance of cortical neurons was assessed from the linear portion of the voltage–current (*V–I*) relationship (square current pulses of 200 ms duration, applied every 1.25 s) (see Fig. 2*Bb*). Because MSNs display prominent inward membrane rectification during injection of large-amplitude negative current pulses (Nisenbaum & Wilson, 1995; Mahon *et al.* 2001, 2004) (Fig. 4*Bb*), their membrane input resistance was measured by the mean ($n = 20$) membrane potential change at the end of hyperpolarizing current pulses of −0.4 nA. The membrane time constant was given by the coefficient of the exponential decay fit of the current-induced hyperpolarization.

Layer 5 cortical cells, located within the barrel cortex, were recorded from the vicinity of the ECoG electrode at the following stereotaxic coordinates: 5.2–8.5 mm anterior to the interaural line, 3.8–5 mm lateral to the midline, and 944–3380 μm under the cortical surface. Some of these cells could be electrophysiologically identified as CS neurons by their antidromic activation (see Fig. 3*A*). To avoid any stimulation of *fibres de passage*, after 3-D reconstruction (not shown) of anterogradely labelled barrel cortex corticofugal axons (Fig. 1*B*, see below for detailed procedures), we identified a striatal sector in which the cortical projections arising from the barrel cortex did not project to other subcortical structures. Accordingly, electrical stimulations were applied rostrally to the level where CS axons enter the ipsilateral striatum, at the following stereotaxic coordinates: 7.3–7.5 mm anterior to the interaural line, 4.6–4.7 mm lateral to the midline, and 4 mm under the brain surface. The striatal stimulations used for antidromic activation (200 μs duration, 4–11 V) were applied with a bipolar concentric electrode (NE-100; Rhodes Medical Instruments, Woodland Hills, CA, USA). The criteria used for identification of antidromic action potentials were their constant latency in response to striatal stimulation and their collision with spontaneously occurring orthodromic action potentials (Fig. 3*A*).

Striatal MSNs and interneurons were recorded in the ipsilateral striatal projection field of the barrel cortex CS neurons (Fig. 1*C*). The corresponding stereotaxic coordinates were as follows: 7–8.5 mm anterior to the interaural line, 4.4–5 mm lateral to the midline, and 3.3–6 mm ventral to the brain surface.

Anatomical procedures and identification of the barrel cortex-related striatal sector

Extracellularly recorded neurons were labelled by juxtacellular injection of Neurobiotin (Pinault, 1996; Paz *et al.* 2007). Briefly, positive current pulses (1–8 nA; 200 ms) were applied at a frequency of 2.5 Hz through the bridge circuit of the amplifier. The current was slowly increased while the electrode was advanced toward the neuron in 1 μm steps until the cell discharge was driven by the injected current. Current pulses were applied for a 10–30 min period to obtain a reliable labelling of neuronal processes. For intracellular recordings, depolarizing current pulses (0.2–1 nA; 200 ms) were applied at a frequency of 0.9 Hz at the end of the recording period. The histochemical methods used to reveal the morphology of intra- and juxtacellularly filled neurons have been described in detail previously (Polack & Charpier, 2006). The position of labelled neurons within the cortex or the striatum was then confirmed using the atlas of Paxinos & Watson (1986).

Extracellular deposits of *Phaseolus vulgaris* Leucoagglutinin (PHA-L) were made into the barrel cortex to determine the site and the pattern of striatal innervations by barrel cortex CS neurons ($n = 2$ experiments). The correct location of the tip of the injection electrode into the barrel cortex (7.3 mm anterior to the interaural line, 5 mm lateral to the midline, and 1.8 mm ventral to the brain surface) (Fig. 1*B*) was confirmed by the recording, at the surface of the injected cortical region, of large-amplitude ERPs evoked by application of air-puffs to the contralateral whiskers (Fig. 1*A*). PHA-L (2.5% in phosphate-buffered saline; Vector Laboratories) was iontophoretically ejected via glass micropipettes (internal tip diameter 8–10 μm) by positive current pulses of 4.5 μA (7 s on/7 s off) for 35–40 cycles. The histological procedures applied to visualize the axons of anterogradely labelled CS neurons are described in detail elsewhere (Degos *et al.* 2008). Axonal terminations in the striatum ipsilateral to the injected barrel cortex (Fig. 1*D*) were observed on a light microscope under brightfield illumination and reconstructed at high-power magnification using the Neurolucida system. The striatal location of CS projections (Fig. 1*C*), as well as their clustered pattern of axonal terminals (Fig. 1*D*), were identical to those described in a detailed previous anatomical study (Alloway *et al.* 1999).

Whisker stimulation

Sensory stimulations, consisting of puffs of compressed air delivered by a picospritzer unit (Picospritzer III, Intracel Ltd, Royston, Herts, UK), were applied through a 1 mm diameter glass pipette placed 15–25 mm rostrolateral from the whiskers. Air puffs (50 ms duration) were given 50 times for each tested intensity (ranging between 8 and 55 p.s.i.) with a low frequency (0.24 Hz) to prevent adaptation of whisker-evoked responses (Chung *et al.* 2002). The intensity of the optimal sensory stimulus, i.e. the minimal air-puff pressure that generated a contralateral ERP of maximal amplitude (100–200 μV), was determined at the beginning of each experiment. Under these conditions, the air-puff stimuli deflected 4–8 whiskers by ~10 deg.

Data acquisition and analysis

Intracellular recordings were obtained under current-clamp conditions using the active bridge mode of an Axoclamp-2B amplifier (Axon Instruments, Union City, CA, USA). Data were digitized and stored on-line with a sampling rate of 25 kHz (intracellular signals), or 3 kHz (ECoG, ERP). Cross-correlograms between subthreshold intracellular activity (1–2 s of continuous recording down-sampled at 3 kHz) and ECoG signal, with the cortical wave as the temporal reference, were calculated using Spike 2 (CED Software; Cambridge Electronic Design, Cambridge, UK).

The amplitude of action potentials was calculated, after averaging 5–10 waveforms, as the potential difference between their voltage threshold, measured as the membrane potential at which the dV/dt exceeded 10 V s^{-1} (Mahon *et al.* 2003), and the peak of the spike waveform. Their total duration was measured as the time between their voltage threshold and the return to the same membrane potential value. The spontaneous firing rate of neurons was calculated from a continuous recording period >10 s.

The latency of intracellular sensory-evoked responses was calculated as the time between the onset of the air-puff stimulus and the foot of the evoked potential. Neuronal events having a shape (rising and decay phases) and/or latency that did not match those of the mean synaptic response obtained after averaging 30–50 trials were not considered as induced by the whisker stimulation and discarded. The amplitude of individual sensory-evoked subthreshold potentials was measured as the voltage difference between the membrane potential at the foot and the peak of the response. The firing probability of neurons in response to whisker deflections was calculated as the ratio between the number of suprathreshold synaptic responses and the total number of sensory-evoked responses.

Numerical values are given as means ± standard error of the mean (S.E.M.). Statistical significances were assessed using, appropriately, Student's *t* tests, the Mann–Whitney rank sum test, the Kruskal–Wallis one-way analysis of variance on ranks or the Levene median test. Statistical analyses were performed with SigmaStat 3.1 (SPSS Inc., Chicago, IL, USA) and curve fitting with Origin 7.0 (OriginLab Corp., Northampton, MA, USA).

Results

Sensory integration in barrel cortex layer 5 CS neurons

We first examined the sensory responses evoked in pyramidal neurons ($n = 65$) located in layer 5 of the barrel cortex, which contains the corticofugal neurons projecting to the dorsolateral striatum (Wright *et al.* 2001; Alloway *et al.* 2006). The depth of intracellular recordings, between 944 and 3380 μm from the cortical surface (1534 ± 48 μm; $n = 65$ cells), suggested that the recorded neurons were exclusively located in layer 5 (Hall & Lindholm, 1974). This was subsequently confirmed by histological analysis of labelled neurons ($n = 3$; Fig. 2*A*), which exhibited the typical morphological features of large-size layer 5 pyramidal neurons of the barrel cortex

(Feldman, 1984; Manns *et al.* 2004; Wilent & Contreras, 2004), including a triangular or ovoid cell body, a prominent apical dendrite extending vertically toward the pial surface and basal dendrites radiating out from the base of the soma.

The electrical membrane properties of recorded cortical neurons included a membrane potential of -64 ± 0.4 mV (range, -70.5 to -57 mV; $n = 65$ cells) (Fig. 2*Ba* and *Cb*), an apparent input resistance (Fig. 2*Ba* and *Bb*) of 22 ± 0.9 MΩ (range, 10.4–40.8 MΩ; $n = 65$ cells) and a membrane time constant (Fig. 2*Ba*) ranging between 3.6 and 18 ms (8 ± 0.3 ms; $n = 65$ cells). Action potential amplitude had a mean value of 65.4 ± 0.8 mV ($n = 65$ cells), with a total duration of 1.4 ± 0.1 ms ($n = 65$ cells), and a voltage threshold of -51.6 ± 0.4 mV (range, -57.5 to -41.6 mV; $n = 65$ cells). In about half of the recorded cells, large-amplitude hyperpolarizing current pulses could induce a depolarizing 'sag' of membrane potential (Fig. 2*Ba*), probably caused by a hyperpolarization-activated inward cationic current (I_h, Breton & Stuart, 2009). The negative current pulse was followed immediately by a post-inhibitory rebound of depolarization (Fig. 2*Ba*, crossed arrows), possibly caused by the slow kinetics of I_h and/or by a low voltage-activated calcium potential. In response to depolarizing current injection, barrel cortex layer 5 neurons responded preferentially with either regular ($n = 30$; Fig. 2*Ba* top) or intrinsic bursting pattern ($n = 35$; Fig. 2*Ba* bottom, arrow). The *V–I* relationship, measured from the early part of the voltage deflection (Fig. 2*Ba*, circles), was linear (Fig. 2*Bb*) and the corresponding firing frequency–current curve followed a sigmoid function (Fig. 2*Bb*), with a maximal firing rate of 48.4 ± 2 Hz ($n = 60$ cells). The membrane potential in all cells showed ongoing oscillatory-like depolarizations, which were correlated with the related ECoG activity and provoked spontaneous firing ranging from 0.05 and 23.5 Hz (Fig. 3*B*). Altogether, these morpho-functional properties are consistent with those already described for rat layer 5 barrel cortex neurons *in vitro* and *in vivo* (Ito, 1992; Gottlieb & Keller, 1997; Zhu & Connors, 1999; Schubert *et al.* 2001, 2006; Manns *et al.* 2004; Breton & Stuart, 2009).

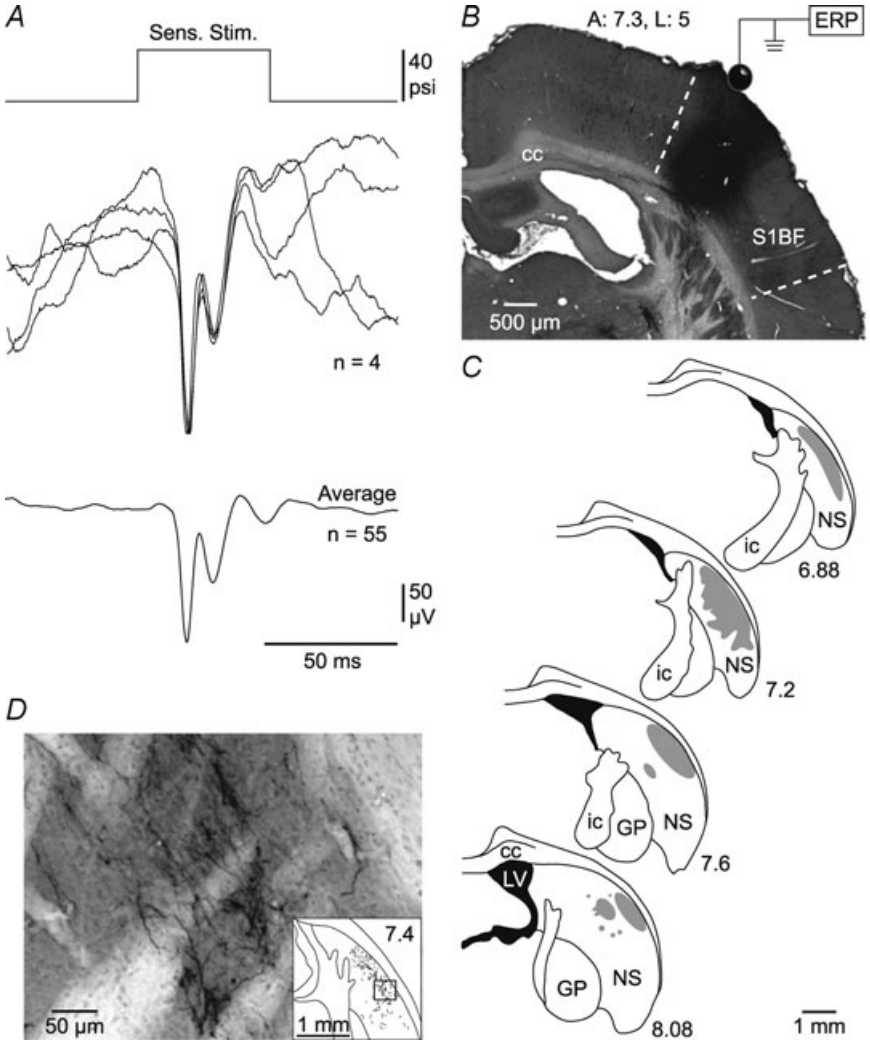

Figure 1. Anatomo-functional characterization of CS projections from barrel cortex
A, average surface ERP (bottom record, $n = 55$ successive trials), and examples of 4 individual records (middle), in response to sensory stimulations (Sens. Stim., air-puffs of 40 p.s.i. applied to the contralateral whiskers) (top trace). *B*, microphotograph of the PHA-L injection site in the barrel cortex (dashed lines, S1BF) at the indicated anterior and lateral positions, and from the cortical field where the ERPs shown in *A* were recorded. *C*, reconstructions of selected coronal sections (at the indicated anterior position) showing the patterns of CS axonal projections (grey areas) within the ipsilateral dorsolateral striatum, which are concordant with those previously described (see Alloway *et al.* 1999; Wright *et al.* 1999). *D*, microphotograph of PHA-L-labelled CS axons, in the striatal sector shown in the inset, exhibiting the classical densely packed clusters of terminals (see Alloway *et al.* 1999). cc, corpus callosum; GP, globus pallidus; LV, lateral ventricle; ic, internal capsule; NS, neostriatum; S1BF, barrel field region of primary somatosensory cortex.

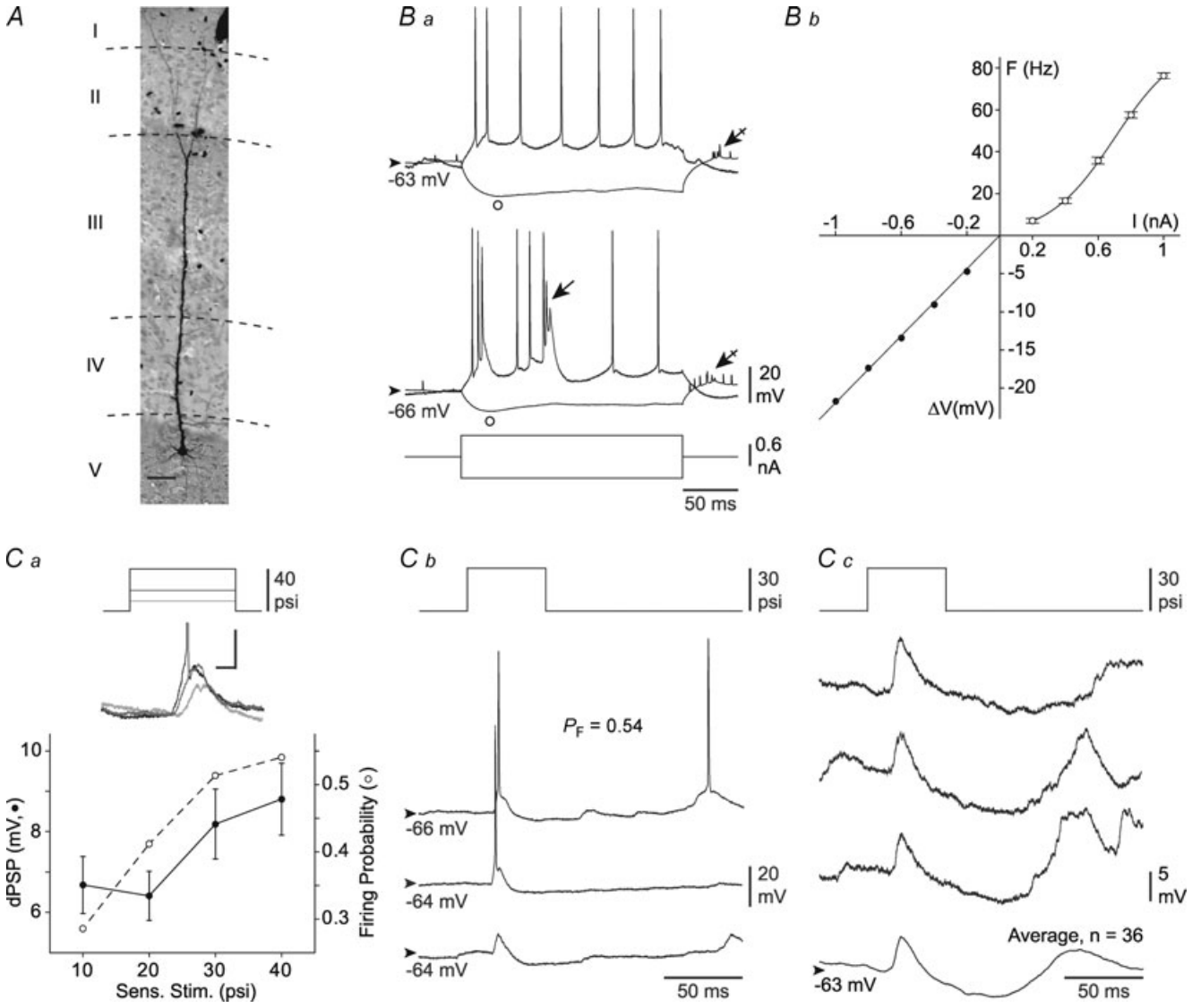

Figure 2. Sensory responses in layer 5 barrel cortex pyramidal cells
A, synthetic projection micrograph (from a 160 μm-thick whole mount) of a Neurobiotin-injected cortical pyramidal neuron whose soma was located in layer 5 of the barrel cortex. Calibration: 50 μm. *B*, electrophysiological properties of layer 5 neurons. *Ba*, intracellular responses (top records) to 200 ms positive and negative current pulses (bottom traces) from a neuron exhibiting a regular spiking pattern (top) and another cell generating intrinsic bursting (oblique arrow, bottom). In both cells, the averaging ($n = 20$) of current-induced hyperpolarizations revealed a sag potential and post-anodal rebound of excitation (oblique crossed arrows). *Bb*, plots of averaged ($n = 20$ trials for each intensity) voltage changes (ΔV, filled circles) and mean firing frequency (F (Hz), open circles) as a function of current intensity. Whereas the *V–I* relation, measured at the time indicated by the open circle in *Ba*, was linear (linear fit; $r^2 = 0.99$), the *F–I* relation followed a sigmoid function ($r^2 = 0.99$). *C*, sensory responses induced in layer 5 barrel cortex cells by contralateral whisker deflection. *Ca*, sensory stimuli (top traces), applied with increasing air-puff pressures, induced depolarizing postsynaptic potentials (dPSPs) that could eventually reach the firing threshold (bottom records). As depicted in the graph below, both dPSPs and firing probability increased in parallel with the intensity of the sensory stimulus ($n = 50$ trials for each intensity). *Cb* and *c*, typical examples of layer 5 cells responding (3 successive individual responses) to air-puffs of same intensity (top traces) with dPSPs that could fired action potentials (*Cb*) or remain subthreshold (*Cc*). In *Cb*, the firing probability (P_F) calculated from 50 trials is indicated and, in *Cc*, the bottom trace represents the average response to 36 stimuli. Here and in the following figures, the values of membrane potential are indicated to the left of the intracellular records.

Air puffs applied to the contralateral whiskers evoked depolarizing postsynaptic potentials (dPSPs) in all recorded layer 5 neurons having a latency ranging between 13 and 29 ms (18.1 ± 0.4 ms, $n = 65$ neurons) (Fig. 2*Ca–c*) and a mean amplitude, calculated from subthreshold responses, of 6.5 ± 0.3 mV (range, 2.5–13 mV). These synaptic properties are similar to those previously measured from layer 5 barrel cortex neurons in response to principal or multiple whiskers stimulation (Moore & Nelson, 1998; Manns *et al.* 2004; Wilent & Contreras, 2004). As exemplified in Fig. 2*Ca*, a progressive increase in air-puff intensity, which enhanced the number of activated whiskers and their deflection magnitude, gradually enhanced the amplitude

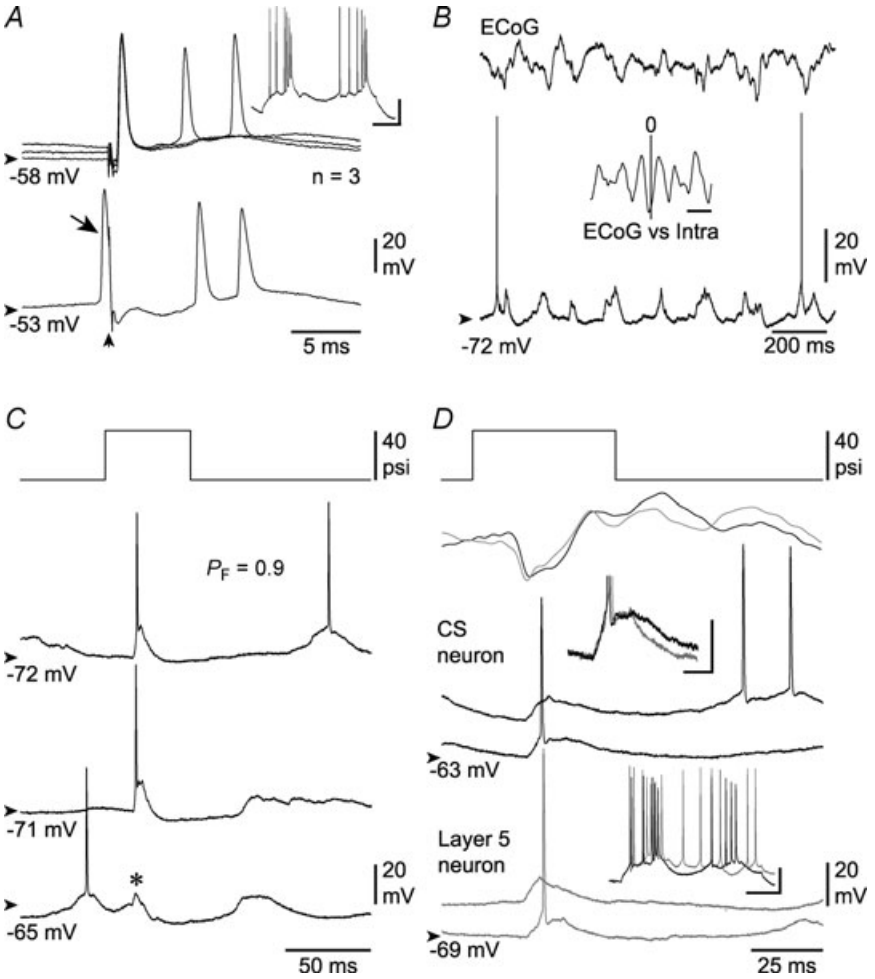

Figure 3. Responses of identified barrel cortex CS neurons to whisker stimulation
A, antidromic identification of CS neurons. Superimposition of 3 successive responses of a barrel cortex layer 5 neuron to electrical stimulations (vertical arrow) of the ipsilateral striatum (top traces). Note the short (0.64 ms), and stable, latency of the first evoked action potential, which was abolished (bottom record) by the collision with a spontaneously occurring orthodromic spike (oblique arrow). This cell displayed an intrinsic bursting pattern (inset) in response to positive current (+0.6 nA) injection (calibrations: 20 mV, 50 ms). *B*, continuous (1.4 s) intracellular recording (bottom record) from an identified CS neuron and the corresponding surface ECoG activity (top trace). The inset depicts the cross-correlation between both signals, using the cortical surface activity as reference (calibration, 200 ms). Note the high correlation between the two oscillatory signals, at a frequency of ~7.5 Hz, with a temporal shift of −18.7 ms. *C*, three successive individual responses in a CS neuron (same as in *B*) to air-puffs applied on the contralateral whiskers (top). Note the high firing probability (P_F) of the cell in response to sensory stimuli despite the occurrence of a small subthreshold dPSP (asterisk), apparently shunted by a prior synaptic activity. *D*, barrel cortex ERPs (top records) and corresponding intracellular responses ($n = 2$) recorded from an identified CS cell (black traces) and an 'unidentified' layer 5 cell (grey traces) in the same experiment and in response to the same sensory stimulus (upper trace). As shown by the expanded records (top inset, calibrations: 10 mV, 10 ms), the latency and shape of suprathreshold sensory responses (spikes are truncated) in both cells were very similar. Injection of a positive current pulse (0.6 nA) generated an intrinsic bursting firing pattern in the two neurons (bottom inset, calibrations: 20 mV, 50 ms).

of subthreshold dPSPs. As previously shown in the same cell type (Manns *et al.* 2004), these multi-whisker synaptic responses could eventually reach action potential threshold with a firing probability that could further increase in parallel with the intensity of the sensory inputs (Fig. 2*Ca*).

In response to iterative optimal whisker stimulation, i.e. with the minimal intensity required to produce the largest ERP in our experimental conditions (see Methods), most of the tested neurons (58 out of 65) could display suprathreshold dPSPs with a probability of evoking an action potential ranging from 0.02 to 1 (0.46 ± 0.04, $n = 58$ neurons) (Fig. 2*Ca* and *b*). In these neurons activated by whisker deflection, the latency of evoked action potentials was 22.3 ± 0.6 ms (range, 15–34 ms, $n = 58$ neurons). In the remaining layer 5 neurons (7 out of 65), sensory stimuli, whatever their intensity, produced dPSPs (maximal amplitude, 5.4 ± 0.3 mV; from 4.2 to 6.3 mV, $n = 7$ neurons) that remained subthreshold for action potential generation (Fig. 2*Cc*). In this limited subset of neurons, the lack of sensory-evoked firing was not due to a defect in their intrinsic excitability since their input resistance (25 ± 2 MΩ, $n = 7$ neurons) and membrane time constant (7.9 ± 0.9 ms, $n = 7$ neurons) were not statistically different to those measured from neurons that could be fired by the sensory stimulus ($P > 0.1$ for each parameter). However, the mean membrane potential of cells that could exhibit suprathreshold responses (-63.5 ± 0.4 mV; $n = 58$ neurons) was slightly, but significantly ($P = 0.03$), more depolarized than that of neurons only displaying subthreshold dPSPs (-66.8 ± 1.4 mV; $n = 7$ neurons), suggesting, as observed in somatosensory cortex neurons (Sachdev *et al.* 2004) and other cortical cells (Azouz & Gray, 1999; Chance *et al.* 2002), that the responsiveness of barrel cortex layer 5 neurons to sensory inputs depends upon the concomitant spontaneous membrane potential fluctuations. Three layer 5 cells displayed ON–OFF responses with a mean firing probability at the OFF potential of 0.2 ± 0.07 (range, 0.05–0.28; $n = 3$ cells). We did not find any substantial differences between sensory-evoked responses recorded from intrinsic bursting and regular spiking neurons.

Some of the recorded layer 5 cortical neurons ($n = 7$) were unequivocally identified as barrel cortex CS cells by their antidromic activation (Fig. 3*A*) from the ipsilateral striatal region receiving axonal projections from the barrel cortex (see Methods and Fig. 1*C*). The average antidromic latency was 0.54 ± 0.10 ms ($n = 7$ cells) (Fig. 3*A*, top traces), corresponding to a conduction velocity of 7.8 ± 1.4 m s^{-1}, a value that is in the upper range of those previously calculated from CS neurons projecting to other striatal sectors (Cowan & Wilson, 1994; Mahon *et al.* 2001). In response to depolarizing current pulses, CS neurons displayed either a regular spiking ($n = 3$) or an intrinsic bursting ($n = 4$) (Fig. 3*A*, inset) pattern. As observed in the whole population of layer 5 neurons, identified CS cells exhibited spontaneous rhythmic membrane depolarizations that were temporally correlated with the barrel cortex ECoG signal (Fig. 3*B*). The mean membrane potential of CS neurons (-65.5 ± 1.7 mV, $n = 7$ neurons), as well as their mean spontaneous firing rate (4.5 ± 2.2 Hz, $n = 7$ neurons), were concordant ($P > 0.15$ for both parameters) with those measured from layer 5 barrel cortex neurons that were not formally identified as CS (membrane potential, -63.6 ± 0.4 mV; firing rate, 5.8 ± 0.8 Hz; $n = 58$ neurons). All CS neurons responded to whisker deflection by dPSPs that could generate action potentials (Fig. 3*C* and *D* middle traces) with a probability of 0.54 ± 0.16 (range, 0.03–0.98, $n = 7$ neurons) and a latency of 25.6 ± 1.7 ms (range, 18.3–33.7 ms, $n = 7$ neurons). These values did not statistically differ ($P > 0.05$ for both values) from those calculated from unidentified layer 5 cells (firing probability, 0.45 ± 0.05, range, 0.02–1; firing latency, 21.8 ± 0.6 ms, range, 15.1–33.8 ms, $n = 51$ neurons) and were similarly distributed. These findings indicate that CS neurons do not provide a distinct functional subset among the barrel cortex layer 5 neurons and suggest that the sensory responsiveness in the overall cortical neuron population recorded in this study is statistically representative of the sensory integration process in CS cells. This assumption is also supported by the single experiment illustrated in Fig. 3*D* in which an identified CS cell (middle traces) and a layer 5 cortical cell not identified as CS (bottom traces) displayed similar sensory responses (top inset) and intrinsic firing patterns (bottom inset).

Morphological and electrophysiological features of barrel cortex-related striatal MSNs

We analysed the morphological and electrophysiological properties of MSNs ($n = 49$) located in the striatal projection field of the barrel cortex. Medium spiny neurons account for the majority of neurons in the striatum (Chang *et al.* 1982) and integrate on their dendritic spines thousands of glutamatergic inputs arising from a large number of converging CS cells (Wilson, 1995*a*; Kincaid *et al.* 1998). Labelled cells (see Methods) (Figs 4*A* and 7*A*), which confirmed the location of recorded neurons within the striatal region receiving inputs from the barrel cortex, displayed the distinctive morphological features of MSNs (Chang *et al.* 1982; Kawaguchi *et al.* 1990). Briefly, they possessed somata of diameter between 10 and 20 μm, with 4–6 ramified primary dendrites densely covered with spines apart from their most proximal regions (Figs 4*A* and 7*A*).

Consistent with their morphological features, intracellularly recorded striatal neurons had the characteristic electrophysiological properties of MSNs

as described *in vitro* and *in vivo* (Kawaguchi *et al.* 1989; Nisenbaum *et al.* 1994; Nisenbaum & Wilson, 1995; Mahon *et al.* 2001, 2003, 2004; Slaght *et al.* 2004). They had a highly polarized membrane potential (-76.1 ± 0.7 mV, from -86.3 to -66.7 mV; $n = 49$), an apparent membrane input resistance of 26.7 ± 1.2 MΩ (range, 12.4–54.5 MΩ; $n = 47$) and a membrane time constant ranging between 5.1 and 18.7 ms (9 ± 0.4 ms; $n = 47$ cells) (Fig. 4*Ba*). The membrane *V–I* relationship consistently displayed a marked inward rectification in response to current pulses of increasing negative intensity (Fig. 4*Bb*, dashed line). Threshold positive current pulses evoked a slow ramp-like membrane depolarization (Fig. 4*Ba*, dashed line) that led to a delay in the first action potential discharge. An increase in the intensity of positive current resulted in a reduction of the first latency and repetitive firing (Fig. 4*Ba*, grey trace). Action potentials of MSNs had an amplitude and duration of 61.8 ± 1 mV and 1.2 ± 0.03 ms ($n = 49$ cells), respectively, and a voltage threshold of -49.4 ± 0.3 mV ($n = 49$ cells). In accordance with their monosynaptic excitatory inputs arising from the barrel cortex, MSNs displayed spontaneous membrane potential fluctuations tightly correlated with the ECoG signal (Fig. 4*C*), which generated a weak and erratic discharge of action potentials (0.6 ± 0.3 Hz; range, 0.01–5.7 Hz; $n = 17$ cells). As expected from their prominent membrane inward rectification (Fig. 4*Bb*), due to a powerful voltage-activated K^+ conductance (Nisenbaum *et al.* 1994; Mahon *et al.* 2004), DC hyperpolarization of MSNs resulted in an attenuation of amplitude of spontaneous synaptic depolarizations (Fig. 4*C*, lowest trace).

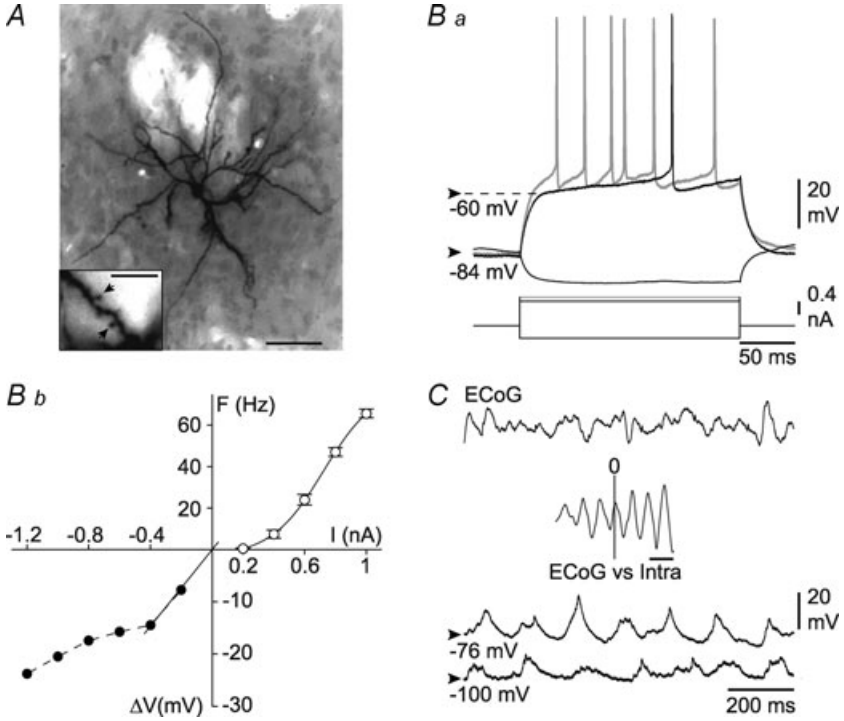

Figure 4. Morpho-functional properties of MSNs located in the striatal projection field of barrel cortex
A, synthetic projection micrograph (from an 80 μm-thick whole mount) of a striatal MSN labelled by intracellular injection of Neurobiotin. This cell exhibited the characteristic morphological features of MSNs (for a detailed description, see Results). *B*, membrane excitability of barrel cortex-related striatal MSNs. *Ba*, voltage changes and firing patterns (top records) in a MSN in response to negative and positive current injections (bottom traces). Note the high membrane polarization at rest and the slow ramp depolarization (dashed line) induced by the threshold current pulse, which led to a delayed firing. Increasing intensity of injected current resulted in a reduction of first spike latency and an augmentation of firing rate (grey record). *Bb*, average voltage changes (ΔV, filled circles) and mean firing rate (*F* (Hz), open circles) plotted as a function of current pulses of increasing intensity. Each data point corresponds to the mean values calculated from 20 successive trials. The *F–I* relation was best fitted by a sigmoid curve ($r^2 = 0.99$) and the *V–I* relation showed a pronounced inward rectification for current pulses more negative than -0.4 nA. *C*, barrel cortex ECoG (upper trace) and simultaneously recorded intracellular activity of a MSN at rest (-76 mV). Both signals are rhythmic and temporally correlated as evidenced by their oscillatory (~7 Hz) cross-correlation (inset, scale bar: 200 ms). Note the attenuation of spontaneous intracellular voltage fluctuations after injection of a continuous negative current (-1 nA; -100 mV), which is consistent with the membrane rectification expressed by MSNs (see *Bb*).

Multi-whisker-evoked responses in striatal MSNs

We analysed the sensory responses evoked in MSNs ($n = 49$) by deflection of contralateral whiskers. Striatal cells could be subcategorized as a function of their responsiveness to an optimal sensory stimulus, which was adjusted in each experiment to provoke the largest cortical response (see Methods).

In 27 MSNs (~55% of tested neurons), air-puffs applied to contralateral whiskers could generate stimulus-dependent responses. These 'responding neurons' exhibited sub- or suprathreshold sensory-evoked dPSPs with a mean latency of 21.0 ± 0.7 ms (range, 14.6–32.6 ms; $n = 27$ neurons). In all responding cells, as observed in layer 5 barrel cortex neurons (see Fig. 2*Ca*), the amplitude of sensory responses increased in parallel with the stimulus intensity (Fig. 5*A*). However, when the air pressure on whiskers was above that of the optimal stimulus, we observed a reduction of the synaptic depolarization (Fig. 5*A*) and a subsequent diminution of the evoked firing (data not shown).

Among the responding MSNs, 19 (39% of tested cells) exhibited, in response to multi-whisker deflection, subthreshold dPSPs with a latency of 21.5 ± 1.0 ms (range, 14.6–32.6 ms; $n = 19$ neurons) (Fig. 5*B*). Their mean amplitude and time-to-peak were of 8.5 ± 0.8 mV (range, 3.3–15.9 mV; $n = 19$ cells) and 8.9 ± 1.2 ms (range, 3.9–22 ms; $n = 19$ cells), respectively. Although amplitude and shape of individual sensory-induced dPSPs showed a high trial-to-trial variability (Fig. 5*B*, upper records), probably due to their polysynaptic origin, the average response (Fig. 5*B*, lower trace) revealed a consistent waveform characterized by a steep initial slope depolarization of 1.1 ± 0.1 V s^{-1} ($n = 19$ cells) and a subsequent slow decaying repolarization lasting between 18 and 108 ms. This synaptic response was followed by an electrical silence (37.4–128 ms of duration) that could be associated with a slight membrane hyperpolarization (1–7 mV), which often preceded a rebound depolarization (Fig. 5*B*, lowest trace).

Whisker stimulation was effective in generating suprathreshold synaptic responses in eight MSNs (16% of recorded cells) (Figs 5*C* and 6*Bb*). In these cells fired by the sensory stimulus, the latency of evoked dPSPs was 19.9 ± 0.7 ms (range, 17.7–22 ms; $n = 8$ neurons), a value similar ($P = 0.3$) to that calculated for MSNs only responding by subthreshold depolarizations. The probability of discharge on depolarizing potentials was relatively low and highly variable among cells (0.17 ± 0.1, range, 0.03–0.35; $n = 8$ neurons) with a latency of action potential ranging from 19.1 to 30.6 ms (mean, 24.3 ± 1.6 ms; $n = 8$ neurons) (Figs 5*C* and 6*Bb*). In these cells that could be fired by whisker deflection, the episodic subthreshold sensory-evoked dPSPs (Figs 5*C* and 6*Bb*, lowest traces) had an amplitude of 8.1 ± 1.2 mV and a time-to-peak of 6.8 ± 0.5 ms ($n = 8$ cells) that did not differ ($P > 0.9$ for each parameter) from those measured in cells showing exclusively subthreshold responses. The current-induced firing in neurons that responded to whisker stimulation by either sub- or suprathreshold potentials was similar, suggesting that the lack of sensory-evoked firing was not caused by an endogenous inability to generate action potentials (Fig. 5*Da vs. Db*). Moreover, the complex waveform of evoked synaptic potentials and subsequent voltage fluctuations recorded in MSNs with subthreshold responses was similar to that observed in neurons that could be activated by sensory inputs (Fig. 5*C vs. B*).

In the remaining 22 MSNs (45% of tested neurons), even though some synaptic depolarizations could occur within the appropriate temporal window after the sensory stimulus (Fig. 6*Aa*, oblique arrows), the averaging of 50 successive trials did not reveal any sensory-evoked response (Fig. 6*Aa* and *Ba* lower traces). It is very unlikely that this absence of whisker-induced response was due to an inability of sensory stimulations to activate CS barrel cortex neurons since the corresponding surface ERP had large amplitude and a standard shape (Fig. 6*Aa*, top record). This assumption is also supported by the single experiment illustrated in Fig. 6*B* in which the same sensory stimulus was unable to generate a response in one MSN (*Ba*) whereas it was effective in inducing suprathreshold potentials in a neighbouring MSN (*Bb*). As shown in Fig. 6*Ab*, the voltage changes and firing patterns induced by current injections in unresponsive neurons were analogous to those recorded in sensory responding MSNs (see Fig. 5*D* for comparison).

The heterogeneous sensory-induced responses recorded in striatal MSNs could, in theory, result from differences in their membrane excitability. To test for this hypothesis, we compared the values of membrane potential, input resistance, membrane time constant, action potential voltage threshold and spontaneous firing rate calculated from MSNs exhibiting suprathreshold responses ($n = 8$) or subthreshold responses ($n = 19$) and those without identified responses ($n = 22$). As shown in the summary histograms in Fig. 6*C*, none of these parameters was found to be significantly different between the three groups of MSNs ($P > 0.05$ for each parameter).

Contribution of chloride-dependent inhibition in sensory integration in MSNs

The lack of sensory response in some of the recorded MSNs, as well as the inability of some of the responding neurons to generate an action potential, is not due to a defect in their intrinsic excitability (see above). Instead, it could result from an insufficient excitatory synaptic drive and/or from a shunting inhibition concomitant with the

sensory-evoked synaptic excitation. To test for a possible inhibitory role of a Cl^--dependent synaptic conductance in the sensory integration in MSNs, we performed intracellular recordings of MSNs with KCl-filled electrodes ($n = 13$ neurons). In such recording conditions, it is expected that the activation of GABA type-A receptors in the membrane MSNs (Wilson, 2007) will cause a dramatic outflow of Cl^- resulting in additional synaptic depolarizations and an increased firing rate (Slaght *et al.* 2004).

Chloride-loaded MSNs were intracellularly filled with Neurobiotin and their morphological features were found to be similar to those of MSNs recorded with KAc-filled electrodes (Fig. 7*A* *vs.* Fig. 4*A*), demonstrating the identity of striatal cells recorded in both conditions. Whereas the membrane potential of MSNs filled with Cl^- was more depolarized (-66.8 ± 1.5 mV, from -74.5 to -55.5 mV; $n = 13$ neurons; $P < 0.001$), their input resistance (29.3 ± 2.2 MΩ; $n = 13$ neurons) and spike threshold (-48.4 ± 0.7 mV; $n = 13$ neurons) remained unchanged ($P > 0.15$ for both parameters) compared to those recorded with KAc electrodes. The presence of depolarizing Cl^--dependent synaptic potentials in the background activity was attested by an uncommonly large amplitude and prolonged spontaneous depolarizations (Fig. 7*B* inset), which were responsible for an elevated firing rate (1.6 ± 0.6 Hz, from 0.03 to 7.1 Hz, $n = 13$ neurons; $P = 0.01$) (Fig. 7*B*).

A remarkable finding was the dramatic increase in the proportion of MSNs responding to sensory stimulation when recorded with KCl-filled electrodes (Fig. 7*D*). In 11 neurons (85% of Cl^--loaded MSNs), whisker deflection provoked dPSPs that occurred with a latency of 24.0 ± 1.2 ms ($n = 11$ neurons). These sensory-evoked responses could evoke action potentials (Fig. 7*Ca*) with a probability of 0.15 (range, 0.05–0.25; $n = 8$ cells) and a latency of 29.7 ± 2.7 ms (range, 22.9–41.6 ms; $n = 8$ cells), or remained subthreshold ($n = 3$ cells) (Fig. 7*Cb*). Interestingly, the time-to-peak of sensory-induced synaptic depolarizations in Cl^--filled MSNs (11.1 ± 1.6 ms; $n = 11$ cells) was slightly but not significantly ($P > 0.05$) longer than that measured from sensory responding MSNs recorded with KAc electrodes (8.3 ± 4.6 ms; $n = 27$ neurons), suggesting the existence of

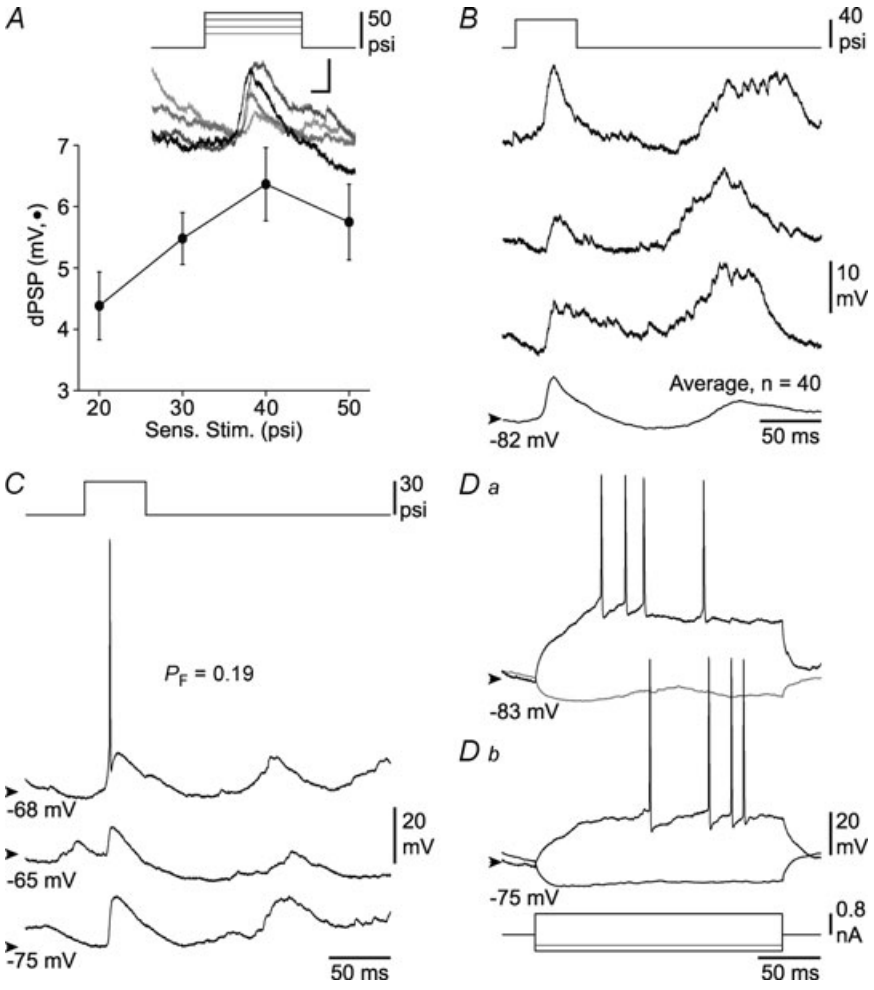

Figure 5. Sensory responses in striatal MSNs
A, air-puffs applied to contralateral whiskers, with increasing pressures (top traces) evoked in the recorded MSN subthreshold dPSPs of variable amplitude (bottom records, calibrations: 5 mV, 10 ms). The graph below depicts the mean amplitude of dPSPs ($n > 22$ trials for each intensity) as a function of the intensity of sensory stimuli (Sens. Stim.). Note the inflection in the amplitude of the sensory response above 40 p.s.i., which corresponded to the stimulus producing the largest response in the corresponding cortical ERP ('optimal stimulus', see Methods). *B*, examples of dPSPs ($n = 3$) and corresponding average potential ($n = 40$ successive trials) evoked in MSNs by a whisker stimulus of 40 p.s.i. (top trace). In this cell, the sensory responses remained subthreshold. *C*, three successive responses in a MSN that could respond to the optimal sensory stimulus (top), by sub- or suprathreshold dPSPs with the indicated firing probability (P_F). *D*, current-induced (bottom) responses recorded from the MSNs shown in *B* (*Da*) and in *C* (*Db*).

a Cl^--dependent synaptic conductance in the initial part of the sensory-evoked response in MSNs.

Our results suggested that contralateral whisker deflection generated a short-latency Cl^--dependent conductance in MSNs that could produce a shunting effect on CS synaptic inputs, a process that could account, at least in part, for the defect of sensory responsiveness in some of the MSNs (see Discussion). Because most MSNs were silent following sensory stimulus, GABAergic interactions between MSNs would participate only moderately in the increase in Cl^- conductance (Wilson, 2007). It might instead originate from a feed-forward activation of intrastriatal GABAergic interneurons, which can be synaptically activated by CS inputs (Ramanathan *et al.* 2002; Mallet *et al.* 2005) and are known to produce a robust Cl^--dependent inhibition able to

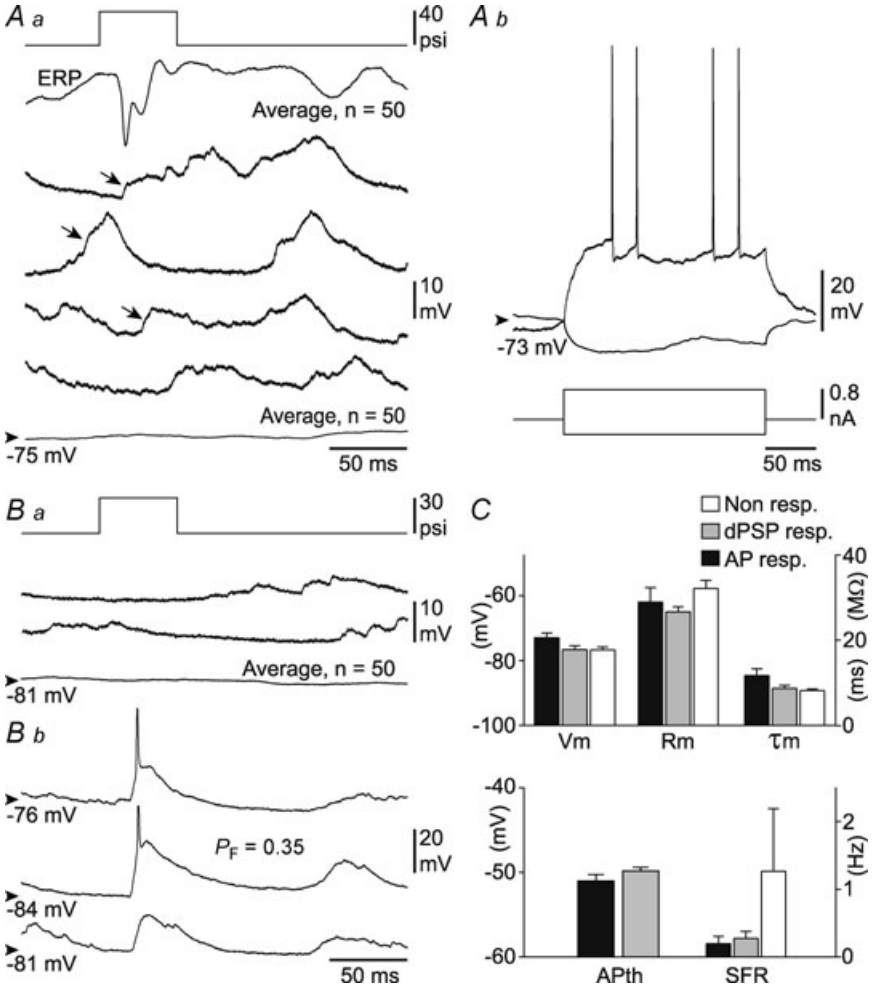

Figure 6. The variability of sensory responses in striatal MSNs is not due to distinct membrane excitability

A, electrophysiological properties of MSNs that did not respond to sensory stimuli. *Aa*, four successive sweeps recorded in a MSN during application of sensory stimuli of 40 p.s.i. Although some synaptic depolarizations occurred in a temporal window compatible with sensory-evoked events (see Fig. 5*B* and *C*), the averaging of 50 successive trials revealed a complete lack of sensory responses (bottom trace). As indicated by the large-amplitude ERP (top average record), the absence of whisker-induced responses in the striatal cell did not result from a deprivation of sensory responsiveness in barrel cortex neurons. *Ab*, current-induced (bottom traces) voltage responses (top) in the MSN shown in *Aa*. Note the similarity of cell excitability compared to that of sensory-reactive MSNs (see Fig. 5*Da* and *Db*). *B*, the same sensory stimulus (top trace) can generate, in two neighbouring MSNs, either no response (*Ba*, two individual records and corresponding average sweep) or dPSPs that can cause spike discharge (*Bb*, three individual records), with the indicated probability firing (P_F). In *Bb*, spikes are truncated for convenience. *C*, pooled histograms of membrane potential (V_m, mV), input resistance (R_m, MΩ), membrane time constant (τ_m, ms), action potential threshold (AP_{th}, mV) and mean spontaneous firing rate (SFR, Hz) calculated from MSNs without sensory responses (Non resp., $n = 22$ neurons) and exhibiting sub- (dPSP resp., $n = 19$ neurons) or suprathreshold responses (AP resp., $n = 8$ neurons). None of these parameters was found to be significantly different between the three neuronal groups ($P > 0.05$ for each parameter).

block the generation of action potentials in MSNs (Wilson, 2007). We tested this hypothesis by performing extracellular recordings of striatal interneurons ($n = 20$) from the same striatal sector where MSNs were recorded. Extracellularly recorded neurons were considered as fast-spiking GABAergic interneurons (Kawaguchi, 1993; Mallet *et al.* 2005; Kreitzer, 2009) on the basis of their short-duration action potentials (0.66 ± 0.04 ms; range, 0.4–0.9 ms; $n = 20$ neurons) (Fig. 7*Ea*, inset) and their morphological properties, revealed after juxtacellular

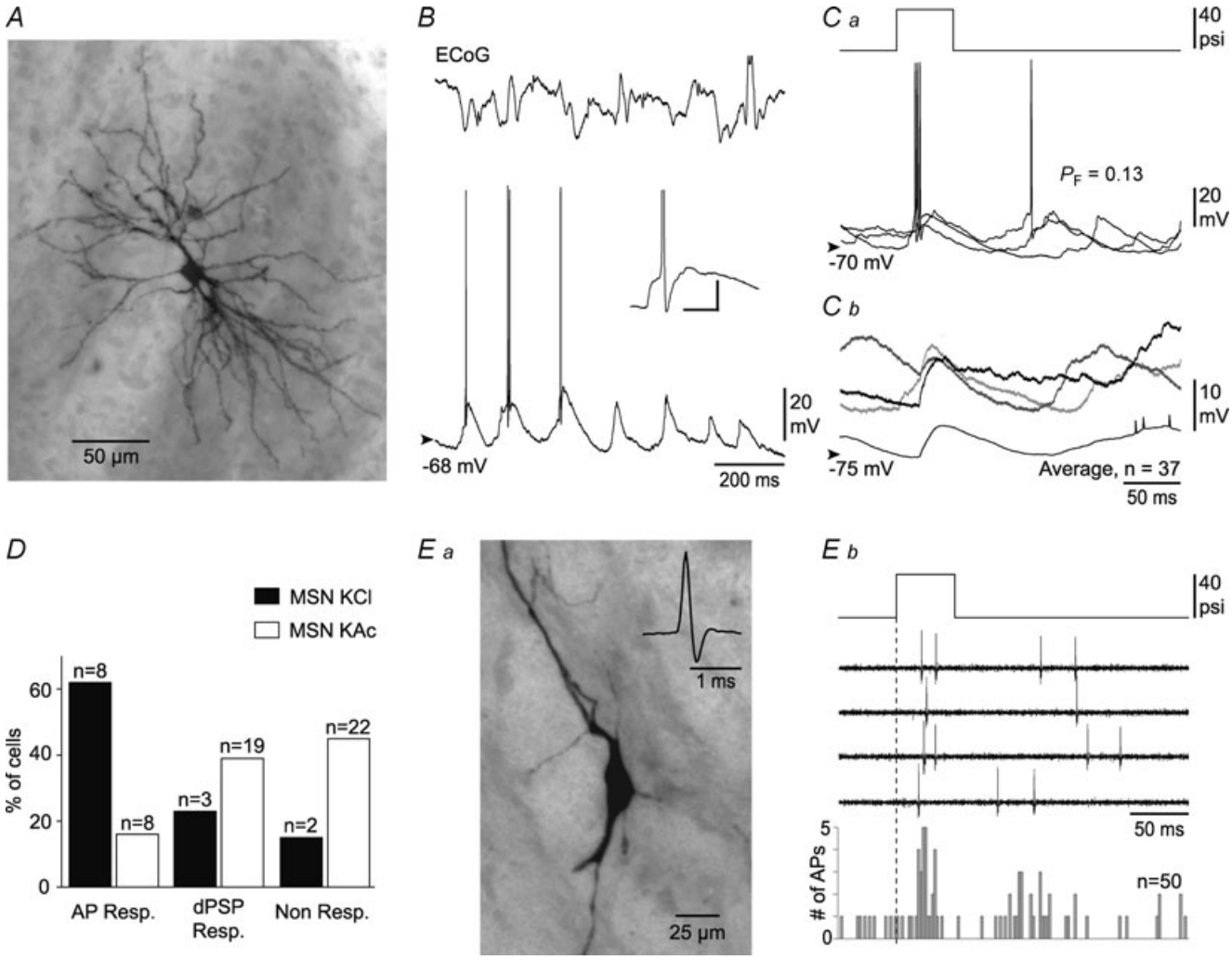

Figure 7. Contribution of Cl^--dependent synaptic inhibition to sensory integration in MSNs
A, synthetic projection micrograph (from a 120 μm-thick whole mount) of a striatal MSN recorded with a KCl electrode and intracellularly labelled with Neurobiotin. *B*, barrel cortex ECoG (upper trace) and simultaneously recorded intracellular activity of a Cl^--loaded MSN (bottom trace). Note the depolarized membrane potential and the elevated firing rate compared to MSN recorded with a KAc electrode (see Fig. 4*C*). As shown by the expanded record (inset, calibrations: 10 mV, 10 ms), the spontaneous firing is caused by large-amplitude and long-duration synaptic potentials, probably resulting from additional Cl^--dependent synaptic depolarizations. *C*, superimposition of 3 successive suprathreshold (*Ca*, the firing probability is indicated) or subthreshold synaptic responses (*Cb*) evoked in two different Cl^--filled MSNs by the same sensory stimulus (top, 40 p.s.i.). The bottom trace in *Cb* represents the average of 37 successive trials. *D*, comparison of the percentage of MSNs (and corresponding number of cells) without sensory responses (Non Resp.), exhibiting subthreshold (dPSP Resp.) or suprathreshold responses (AP Resp.) when recorded with KAc or KCl electrodes. *E*, activation of presumed striatal GABAergic interneurons by whisker deflection. *Ea*, microphotograph of a putative GABAergic striatal interneuron labelled by juxtacellular injection of Neurobiotin. This cell exhibited the morphological features (for a detailed description, see Results) of striatal interneurons with expanded dendritic field (see Kawaguchi, 1993). The inset shows the short-duration (0.58 ms) extracellular spike of the labelled neuron. *Eb*, four successive extracellular sensory responses of a putative GABAergic interneuron and corresponding post-stimulus time histogram of action potential discharges (50 collected sweeps, bin = 2 ms). The vertical dashed line indicates the onset of the air-puffs (top).

injection of Neurobiotin (see Methods), including oval somata of ∼15 μm diameter and 3–5 smooth primary dendrites giving rise to restricted or extended dendritic arborization (Fig. 7*Ea*) (Kawaguchi, 1993). Six striatal interneurons (30% of recorded cells) responded with high reliability to whisker deflection by 1–3 action potentials (Fig. 7*Eb*). The latency of the first sensory-evoked spike was 20.6 ± 1.9 ms ($n = 6$ cells) (Fig. 7*Eb*).

Differential sensory integration in CS neurons and MSNs

Our *in vivo* intracellular recordings revealed that barrel cortex layer 5 neurons, including identified CS cells, responded with high reliability to contralateral multi-whisker deflection, most cortical neurons (89% of recorded cells) exhibiting sensory-evoked dPSPs that could elicit spike discharge with a mean probability of 0.46 (Fig. 8*A* and *B*). In contrast, the sensory integration in the corresponding postsynaptic striatal MSNs was less secure with about 45% of neurons not showing any response to whisker deflection and 55% of cells exhibiting evoked dPSPs, which could generate action potentials in only ∼30% of the responding neurons (Fig. 8*A*). When MSNs could be activated by whisker stimulations their firing was delayed by ∼2 ms compared to the sensory-evoked discharge in cortical cells, a value that is compatible with the monosynaptic connectivity between the two cell populations (see Discussion). However, the firing probability of responding MSNs was significantly lower than that of layer 5 cortical cells ($P < 0.05$) (Fig. 8*B*) while the corresponding temporal dispersion of firing latencies in both neuronal sets was similar ($P > 0.1$) (Fig. 8*B*).

Altogether, this statistical comparison between all neurons recorded in the layer 5 barrel cortex and in the corresponding somatosensory striatum suggested that the propagation of sensory responses from cortex to striatum resulted in a decrease in the number of responding neurons and a reduction in the firing probability of neurons that could be activated. This was directly confirmed by further analysing individual experiments in which both layer 5 barrel cortex cells and MSNs were recorded and submitted to the same sensory stimulus ($n = 17$ experiments) (Fig. 8*Ca* and *Cb*). As illustrated by the single experiment shown in Fig. 8*Ca*, identical sensory stimuli could reliably evoke suprathreshold responses in a barrel cortex layer 5 cell (firing probability = 0.7) whereas they generated subthreshold dPSPs in a MSN and were inefficient at inducing any response in another MSN. The pooled representation of sensory responses recorded from the same experiments in barrel cortex layer 5 neurons and striatal MSNs (Fig. 8*Cb*) demonstrated that, for a given multi-whisker deflection, the quasi-totality of cortical cells were activated (29 out of 32; 91%) whereas most MSNs displayed subthreshold responses (12 out of 33; 36%) or were unaffected (15 out of 33; 45%) by the sensory stimulus. In this set of experiments, in which the relative timing of cortical and striatal sensory responses could be directly compared, the mean latencies of whisker-mediated cortical spikes and synaptic depolarizations in MSNs were 20.9 ± 0.8 ms ($n = 21$ layer 5 neurons) and 21.6 ± 1.0 ms ($n = 18$ MSNs), respectively, corresponding to a fast CS transmission in accordance with the propagation time of CS action potentials (∼0.6 ms, see above) in addition to an excitatory monosynaptic delay (∼0.3 ms; Eccles, 1964).

To confirm that the results presented above are not conditional upon a specific anaesthetic procedure, we performed an additional set of experiments in rats ($n = 13$) anaesthetized with fentanyl (see Methods), which induces a relatively desynchronized background ECoG (Mahon *et al.* 2001; Polack & Charpier, 2006). Barrel cortex layer 5 neurons ($n = 12$) and related MSNs ($n = 15$), recorded under fentanyl, had similar electrical membrane properties and current-induced firing patterns to those recorded from pentobarbital-anaesthetized rats (Supplemental Fig. 1*Ca* and *Cb*, available online only). Among cortical cells, contralateral multi-whisker deflection induced dPSPs having a mean latency of 14.8 ± 0.6 ms; $n = 12$ neurons), which were efficient at generating action potentials in 92% of recorded cells (mean firing probability = 0.38 ± 0.09; $n = 11$ neurons) (Supplemental Fig. 1*A* top and *D*). As observed under pentobarbital, only a limited proportion of MSNs ($n = 8$; 53% of recorded neurons) could exhibit whisker-mediated dPSPs (Supplemental Fig. 1*B* and *D*), which had a mean latency of 22.7 ± 1.6 ms ($n = 8$ neurons) and were able to produce suprathreshold responses in only 20% of recorded MSNs ($n = 3$) (Supplemental Fig. 1*B* and *D*) with a low firing probability (from 0.02 to 0.2). In the remaining MSNs ($n = 7$; 47% of recorded neurons), no sensory response could be detected (Supplemental Fig. 1*A* bottom and *D*). These results, similar to those obtained under pentobarbital anaesthesia (Fig. 8*A* *vs.* Supplemental Fig. 1*D*), demonstrate that the differential sensory integration in CS neurons and MSNs does not depend upon specific experimental conditions and occurs during various profiles of cortical activities.

Discussion

The main findings of the present study, which provides the first description of the intracellular sensory events generated in the corticostriatal pathway by contralateral whisker deflection, are as follows: (1) layer 5 barrel cortex neurons, including identified CS cells

projecting to the dorsolateral striatum, responded to sensory stimuli by dPSPs that mostly caused cell firing; (2) about 55% of recorded striatal MSNs displayed sensory-evoked depolarizations that could generate action potentials in a third of these neurons; (3) the remaining MSNs did not exhibit any detectable electrical events in response to whisker stimulation; (4) the proportion of sensory-responding MSNs was dramatically increased by intracellular injection of Cl^-, suggesting that an inhibitory GABA type-A synaptic conductance is responsible, at least in part, for the relative unreliability of sensory-evoked responses in MSNs; and (5) putative striatal GABAergic interneurons could be activated by whisker stimulation, a process that may account for the Cl^--dependent synaptic conductance observed in MSNs. These results suggest that the propagation of sensory flow through the CS pathway following whisker deflection results in a partial loss or a refinement of sensory information in the striatum.

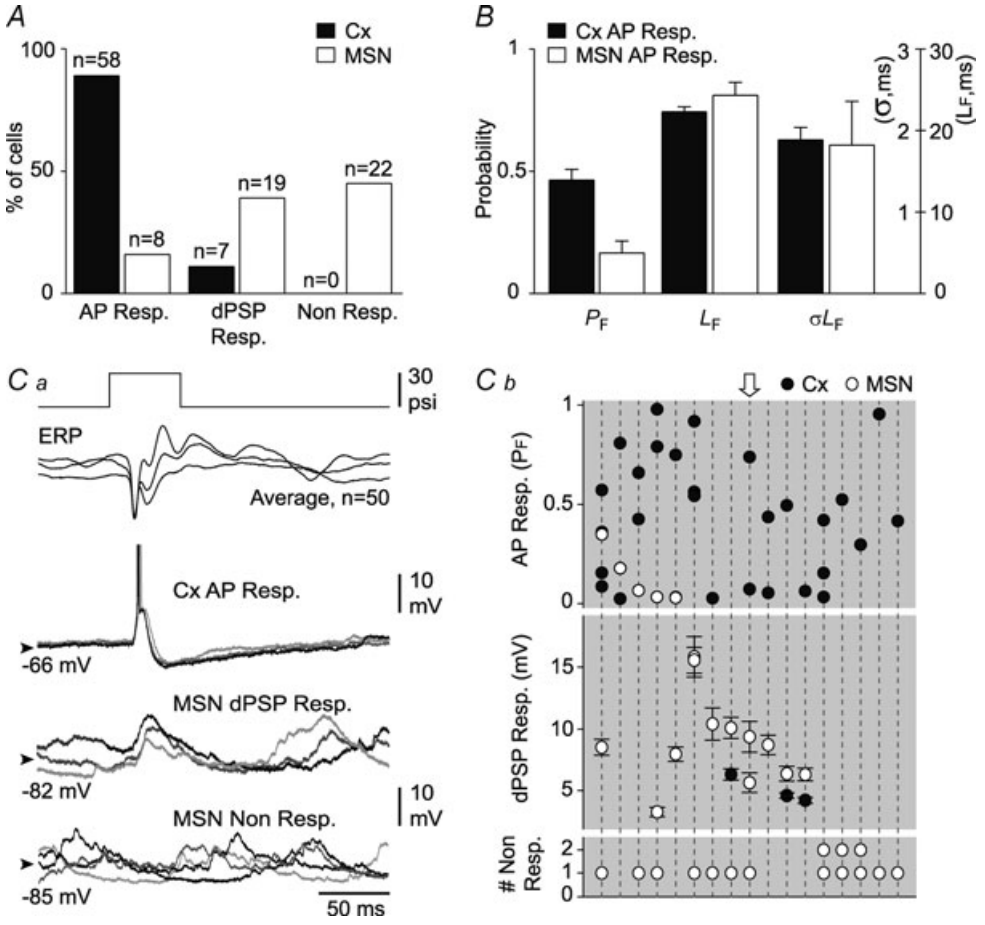

Figure 8. Comparison of sensory-mediated responses in barrel cortex layer 5 cells and MSNs
A, comparison of the percentage of MSNs and barrel cortex layer 5 neurons (Cx), and corresponding number of recorded cells, exhibiting no detectable sensory response (Non Resp.), subthreshold (dPSP Resp.) or suprathreshold responses (AP Resp.). *B*, summary histograms of probability of firing (P_F), latency of firing (L_F) and corresponding values of standard deviation (σL_F), calculated from MSNs ($n = 8$) and cortical neurons ($n = 58$) that could be fired by the sensory stimulus. Only the probability of firing was significantly different between the two groups ($P = 0.03$). *C*, comparison of sensory responses evoked in layer 5 cortical cells and MSNs recorded during the same experiment. *Ca*, averaged ERPs (top records) and superimposition ($n = 3$) of corresponding intracellular activities recorded, during the same experiment and following the same whisker deflection, from a layer 5 barrel cortex neuron responding by suprathreshold responses (Cx AP Resp., $P_F = 0.74$) (spikes are truncated), a MSN responding by subthreshold depolarizations (MSN dPSP Resp.) and another MSN without detectable response (MSN Non Resp.). *Cb*, synthetic representation of sensory responses in barrel cortex layer 5 neurons (Cx) and MSNs that were recorded during the same experiment and after application of identical whisker stimulations ($n = 17$ experiments). Each vertical dashed line corresponds to a single experiment and the corresponding values of dPSP amplitude, probability of firing, as well as the number of unresponsive neurons (Non Resp.) are indicated. The vertical arrow indicates the experiment illustrated in *Ca*.

Sensory activation of barrel cortex CS neurons

Our *in vivo* intracellular recordings in the barrel cortex were exclusively made from layer 5 where the somata of corticofugal neurons projecting to the dorsolateral striatum are located (Wright *et al.* 1999, 2001; Alloway *et al.* 2006). Although only a limited number of cells (11% of recorded neurons) were antidromically identified as CS cells, we did not find any significant difference between the electrophysiological features of identified and unidentified CS cells, including their membrane properties and sensory-evoked responses, which are also similar to those previously described from barrel cortex layer 5 pyramidal neurons *in vivo* (Zhu & Connors 1999; Schubert *et al.* 2001, 2006; Manns *et al.* 2004; Wilent & Contreras, 2004).

Consistent with the local optimal surface ERPs, all recorded cortical neurons showed a highly reliable sensory-evoked synaptic activation, which could originate from various thalamocortical and intracortical networks activated by whisker deflection (Brecht, 2007). Superficial layer 5 pyramids receive excitatory thalamic input from the medial posterior nucleus (Lu & Lin, 1993), they are interconnected (Schubert *et al.* 2006) and innervated by axonal arbors from layer 4 excitatory spiny stellate cells (Brecht & Sakmann, 2002; Schubert *et al.* 2006). In contrast, the large pyramidal cells in the deeper part of layer 5 integrate excitatory inputs from ventral posteromedial thalamic projections (Lu & Lin, 1993), axonal ramifications of layer 2–3 neurons (Lübke *et al.* 2003) and are also reciprocally connected (Markram *et al.* 1997). These glutamatergic, thalamic and intracortical inputs probably account for the early part of evoked dPSPs. It is also probable that this fast sensory-induced excitation is partially overlapped by a fast inhibitory synaptic conductance (Wilent & Contreras, 2004), possibly resulting from the activation of intracortical GABAergic interneurons by thalamocortical projections (Swadlow, 2003). It is likely that this surrounding inhibition, which would be amplified by multiple whisker activation (Mirabella *et al.* 2001; Ego-Stengel *et al.* 2005), partly governs the probabilistic firing of CS cells following sensory stimulation and is responsible for sublinear summation of responses when increasing the number of coincident inputs (Mirabella *et al.* 2001) (see Fig. 2*Ca*).

Origin and heterogeneity of whisker-mediated responses in striatal MSNs

A striking result is the heterogeneous and insecure whisker-mediated sensory responsiveness of MSNs recorded within the striatal projection field of the barrel cortex, which contrasts with the high reliability of sensory integration in CS neurons. Notably, the lack of correlated synaptic depolarization between CS neurons and related MSNs (∼45% of recorded MSNs) as well as between neighbouring MSNs was not previously reported (Stern *et al.* 1998; Charpier *et al.* 1999; Mahon *et al.* 2001). Whereas 89% of layer 5 cortical cells, including all of the identified CS neurons, displayed suprathreshold dPSPs in response to whisker stimulation, only 55% of MSNs exhibited whisker-mediated dPSPs that could cause, in only ∼30% of these responding neurons, action potential discharge. Such an imbalance between the firing rates of CS cells and MSNs is consistent with what was previously described *in vivo* during anaesthetic-dependent rhythmic spontaneous activities (Stern *et al.* 1997; Mahon *et al.* 2001, 2004).

It is likely that the whisker-evoked depolarizations in MSNs are mainly due to the activation of their barrel cortex CS afferents. First, glutamatergic CS projections provide the major source of synaptic contacts onto the dendrites of MSNs (Kincaid *et al.* 1998), including those located in the barrel cortex-related striatal sector (Wright *et al.* 1999, 2001; Alloway *et al.* 1999, 2006), and are known to sculpt their spontaneous membrane depolarizations (Wilson, 1995*a*; Wilson & Kawaguchi, 1996; Stern *et al.* 1997; Charpier *et al.* 1999; Mahon *et al.* 2001, 2004). Second, the mean delay between whisker-mediated cortical action potentials and synaptic depolarizations in MSNs, measured from the different couples ($n = 33$ from 17 experiments) of cortical and striatal cells recorded in the same experiment and in response to identical multi-whisker deflection, was 1.6 ± 1.1 ms, a value consistent with monosynaptic transmission and in accordance with the fast propagation of the CS action potentials we measured. Third, there is no identified direct projection from whisker-related thalamic nuclei to the dorsolateral striatum (Smith *et al.* 2004). Finally, the temporal sequence of whisker-mediated synaptic events in MSNs resembles the one induced by electrical stimulation of ipsilateral CS neurons (Charpier *et al.* 1999; Mahon *et al.* 2003). However, the possibility is not excluded that the primary motor and secondary somatosensory cortical areas, which converge on the somatosensory striatum (Alloway *et al.* 2006) and could be activated by whisker stimulation (Chakrabarti & Alloway, 2006; Ferezou *et al.* 2007), participate in the sensory-evoked responses in MSNs.

The heterogeneous sensory events in MSNs could originate from different, and possibly synergistic, cellular, synaptic and network mechanisms. It is very unlikely that all non-responding MSNs were located in a striatal sector that did not receive whisker-induced CS inputs since it was possible to record, in the same animal and following identical stimuli, neighbouring MSNs exhibiting subthreshold dPSPs, suprathreshold potentials or no response (see Fig. 8*Ca* and *Cb*). However, given the partial somatotopic representation of the barrel cortex in the striatum (Alloway *et al.* 1999), we cannot

exclude the possibility that some unresponsive MSNs were situated between the clustered axonal terminals of stimulated CS neurons. More probably, the absence of a whisker-mediated striatal response could result from two types of shunting inhibition. First, the relatively low input resistance and short time constant of MSNs membrane (Nisenbaum & Wilson, 1995; Wilson, 1995*a,b*; Mahon *et al.* 2004; this study), which is caused by a powerful voltage-gated K^+-dependent membrane conductance (Nisenbaum & Wilson, 1995), would filter out small dendritic synaptic events, making them undetectable at the somatic level. Second, as demonstrated by the dramatic increase in the number of responsive MSNs after intracellular injection of Cl^-, together with the sensory-evoked firing of putative striatal GABAergic interneurons, it is likely that whisker deflection produces a cortex-mediated activation of intrastriatal GABAergic interneurons (Mallet *et al.* 2005) that, in turn, produce a Cl^--dependent shunting inhibition of excitatory synaptic potentials in MSNs (Slaght *et al.* 2004). This would demonstrate a functional role of feed-forward inhibition during striatal sensory integration.

About half the MSNs were synaptically excited by the multi-whisker deflection. These neurons were probably located in the striatal spot receiving convergent inputs from the CS neurons activated by the sensory stimulation. However, most of these cells responded with synaptic depolarizations that could not reach spike threshold. This could be due to the large voltage drop required to fire MSNs from their resting potential and the activation of inhibitory voltage-gated K^+-dependent conductances acting close to action potential threshold (Nisenbaum *et al.* 1994; Nisenbaum & Wilson, 1995). It is also probable that the activation of striatal GABAergic interneurons produces a shunting inhibition that limits synaptic depolarization positive to the equilibrium potential of Cl^- and, consequently, prevents firing in most MSNs.

Functional implication

It is proposed that the dorsolateral striatum is crucially involved in the control of sensorimotor tasks via the integration, and complex processing, of convergent inputs from functionally related and interconnected somatosensory and motor cortical areas (Flaherty & Graybiel, 1994, 1995; Alloway *et al.* 2006). Taken together, our findings indicate that striatal MSNs located within the projection field of barrel cortex respond differentially to multiple whisker deflection. This process, probably governed by subtle interplay between cortical synaptic inputs, intrastriatal inhibitory networks and the membrane properties of MSNs (see above), might allow a selection or a refinement of 'contextual-dependent' barrel cortex information in the striatum by rejecting combinations of whisker movement that are functionally irrelevant during a given sensorimotor task. The whisker-sensitive MSNs also integrate additional somatosensory and motor information arising from convergent secondary somatosensory and primary motor cortices (Alloway *et al.* 2006). Accordingly, the firing of whisker-related MSNs will be further selected and facilitated when cortical areas are co-activated, either synchronously or in close temporal sequence, thereby encoding specific sets of CS networks that are functionally significant during somaesthetic-guided behaviours.

References

Alloway KD, Crist J, Mutic JJ & Roy SA (1999). Corticostriatal projections from rat barrel cortex have an anisotropic organization that correlates with vibrissal whisking behavior. *J Neurosci* **19**, 10908–10922.

Alloway KD, Lou L, Nwabueze-Ogbo F & Chakrabarti S (2006). Topography of cortical projections to the dorsolateral neostriatum in rats: multiple overlapping sensorimotor pathways. *J Comp Neurol* **499**, 33–48.

Azouz R & Gray CM (1999). Cellular mechanisms contributing to response variability of cortical neurons *in vivo*. *J Neurosci* **19**, 2209–2223.

Barnes TD, Kubota Y, Hu D, Jin DZ & Graybiel AM (2005). Activity of striatal neurons reflects dynamic encoding and recoding of procedural memories. *Nature* **437**, 1158–1161.

Brecht M (2007). Barrel cortex and whisker-mediated behaviors. *Curr Opin Neurobiol* **17**, 408–416.

Brecht M & Sakmann B (2002). Dynamic representation of whisker deflection by synaptic potentials in spiny stellate and pyramidal cells in the barrels and septa of layer 4 rat somatosensory cortex. *J Physiol* **543**, 49–70.

Breton JD & Stuart GJ (2009). Loss of sensory input increases the intrinsic excitability of layer 5 pyramidal neurons in rat barrel cortex. *J Physiol* **587**, 5107–5119.

Brown LL, Feldman SM, Smith DM, Cavanaugh JR, Ackermann RF & Graybiel AM (2002). Differential metabolic activity in the striosome and matrix compartments of the rat striatum during natural behaviors. *J Neurosci* **22**, 305–314.

Brown LL, Hand PJ & Divac I (1996). Representation of a single vibrissa in the rat neostriatum: Peaks of energy metabolism reveal a distributed functional module. *Neuroscience* **75**, 717–728.

Carelli RM & West MO (1991). Representation of the body by single neurons in the dorsolateral striatum of the awake, unrestrained rat. *J Comp Neurol* **309**, 231–249.

Chakrabarti S & Alloway KD (2006). Differential origin of projections from SI barrel cortex to the whisker representations in SII and MI. *J Comp Neurol* **498**, 624–636.

Chance FS, Abbott LF & Reyes AD (2002). Gain modulation from background synaptic input. *Neuron* **35**, 773–782.

Chang HT, Wilson CJ & Kitai ST (1982). A Golgi study of rat neostriatal neurons: light microscopic analysis. *J Comp Neurol* **208**, 107–126.

Charpier S, Mahon S & Deniau JM (1999). *In vivo* induction of striatal long-term potentiation by low-frequency stimulation of the cerebral cortex. *Neuroscience* **91**, 1209–1222.

Chung S, Li X & Nelson SB (2002). Short-term depression at thalamocortical synapses contributes to rapid adaptation of cortical sensory responses in vivo. *Neuron* **34**, 437–446.

Cowan RL & Wilson CJ (1994). Spontaneous firing patterns and axonal projections of single corticostriatal neurons in the rat medial agranular cortex. *J Neurophysiol* **71**, 17–32.

Degos B, Deniau JM, Le Cam J, Mailly P & Maurice N (2008). Evidence for a direct subthalamo-cortical loop circuit in the rat. *Eur J Neurosci* **27**, 2599–2610.

Deniau JM, Menetrey A & Charpier S (1996). The lamellar organization of the rat substantia nigra pars reticulata: segregated patterns of striatal afferents and relationship to the topography of corticostriatal projections. *Neuroscience* **73**, 761–781.

Drummond GB (2009). Reporting ethical matters in *The Journal of Physiology*: standards and advice. *J Physiol* **587**, 713–719.

Eccles JC (1964). *The Physiology of Synapses*. Springer-Verlag, Berlin.

Ego-Stengel V, Mello e Souza T, Jacob V & Shulz DE (2005). Spatiotemporal characteristics of neuronal sensory integration in the barrel cortex of the rat. *J Neurophysiol* **93**, 1450–1467.

Feldman MD (1984). Morphology of the neocortical pyramidal neuron. In *Cerebral cortex*, ed. Peters A & Jones EG, pp. 123–200. Plenum, New York.

Ferezou I, Haiss F, Gentet LJ, Aronoff R, Weber B & Petersen CC (2007). Spatiotemporal dynamics of cortical sensorimotor integration in behaving mice. *Neuron* **56**, 907–923.

Flaherty AW & Graybiel AM (1994). Input-output organization of the sensorimotor striatum in the squirrel monkey. *J Neurosci* **14**, 599–610.

Flaherty AW & Graybiel AM (1995). Motor and somatosensory corticostriatal projection magnifications in the squirrel monkey. *J Neurophysiol* **74**, 2638–2648.

Gottlieb JP & Keller A (1997). Intrinsic circuitry and physiological properties of pyramidal neurons in rat barrel cortex. *Exp Brain Res* **115**, 47–60.

Graybiel AM (2008). Habits, rituals, and the evaluative brain. *Annu Rev Neurosci* **31**, 359–387.

Graybiel AM, Aosaki T, Flaherty AW & Kimura M (1994). The basal ganglia and adaptive motor control. *Science* **265**, 1826–1831.

Hall RD & Lindholm EP (1974). Organization of motor and somatosensory neocortex in the albino rat. *Brain Res* **66**, 23–38.

Ito M (1992). Simultaneous visualization of cortical barrels and horseradish peroxidase-injected layer 5b vibrissa neurones in the rat. *J Physiol* **454**, 247–265.

Kawaguchi Y (1993). Physiological, morphological, and histochemical characterization of three classes of interneurons in rat neostriatum. *J Neurosci* **13**, 4908–4923.

Kawaguchi Y, Wilson CJ & Emson PC (1989). Intracellular recording of identified neostriatal patch and matrix spiny cells in a slice preparation preserving cortical inputs. *J Neurophysiol* **62**, 1052–1068.

Kawaguchi Y, Wilson CJ & Emson PC (1990). Projection subtypes of rat neostriatal matrix cells revealed by intracellular injection of biocytin. *J Neurosci* **10**, 3421–3438.

Kincaid AE, Zheng T & Wilson CJ (1998). Connectivity and convergence of single corticostriatal axons. *J Neurosci* **18**, 4722–4731.

Kreitzer AC (2009). Physiology and pharmacology of striatal neurons. *Annu Rev Neurosci* **32**, 127–147.

Lu SM & Lin RC (1993). Thalamic afferents of the rat barrel cortex: a light- and electron-microscopic study using *Phaseolus vulgaris* leucoagglutinin as an anterograde tracer. *Somatosens Mot Res* **10**, 1–16.

Lübke J, Roth A, Feldmeyer D & Sakmann B (2003). Morphometric analysis of the columnar innervation domain of neurons connecting layer 4 and layer 2/3 of juvenile rat barrel cortex. *Cereb Cortex* **13**, 1051–1063.

Mahon S, Deniau JM & Charpier S (2001). Relationship between EEG potentials and intracellular activity of striatal and cortico-striatal neurons: an *in vivo* study under different anesthetics. *Cereb Cortex* **11**, 360–373.

Mahon S, Deniau JM & Charpier S (2003). Various synaptic activities and firing patterns in cortico-striatal and striatal neurons in vivo. *J Physiol Paris* **97**, 557–566.

Mahon S, Deniau JM & Charpier S (2004). Corticostriatal plasticity: life after the depression. *Trends Neurosci* **27**, 460–467.

Mallet N, Le Moine C, Charpier S & Gonon F (2005). Feedforward inhibition of projection neurons by fast-spiking GABA interneurons in the rat striatum *in vivo*. *J Neurosci* **25**, 3857–3869.

Manns ID, Sakmann B & Brecht M (2004). Sub- and suprathreshold receptive field properties of pyramidal neurones in layers 5A and 5B of rat somatosensory barrel cortex. *J Physiol* **556**, 601–622.

Markram H, Lübke J, Frotscher M, Roth A & Sakmann B (1997). Physiology and anatomy of synaptic connections between thick tufted pyramidal neurones in the developing rat neocortex. *J Physiol* **500**, 409–440.

Mirabella G, Battiston S & Diamond ME (2001). Integration of multiple-whisker inputs in rat somatosensory cortex. *Cereb Cortex* **11**, 164–170.

Moore CI & Nelson SB (1998). Spatio-temporal subthreshold receptive fields in the vibrissa representation of rat primary somatosensory cortex. *J Neurophysiol* **80**, 2882–2892.

Nisenbaum ES & Wilson CJ (1995). Potassium currents responsible for inward and outward rectification in rat neostriatal spiny projection neurons. *J Neurosci* **15**, 4449–4463.

Nisenbaum ES, Xu ZC & Wilson CJ (1994). Contribution of a slowly inactivating potassium current to the transition to firing of neostriatal spiny projection neurons. *J Neurophysiol* **71**, 1174–1189.

Paxinos G & Watson C (1986). *The Brain in Stereotaxic Coordinates*. Academic Press, Sydney.

Paz JT, Chavez M, Saillet S, Deniau JM & Charpier S (2007). Activity of ventral medial thalamic neurons during absence seizures and modulation of cortical paroxysms by the nigrothalamic pathway. *J Neurosci* **27**, 929–941.

Pennartz CM, Berke JD, Graybiel AM, Ito R, Lansink CS, van der Meer M, Redish AD, Smith KS & Voorn P (2009). Corticostriatal interactions during learning, memory processing, and decision making. *J Neurosci* **29**, 12831–12838.

Petersen CC (2007). The functional organization of the barrel cortex. *Neuron* **56**, 339–355.

Pinault D (1996). A novel single-cell staining procedure performed in vivo under electrophysiological control: morpho-functional features of juxtacellularly labeled thalamic cells and other central neurons with biocytin or Neurobiotin. *J Neurosci Methods* **65**, 113–136.

Polack PO & Charpier S (2006). Intracellular activity of cortical and thalamic neurones during high-voltage rhythmic spike discharge in Long-Evans rats *in vivo*. *J Physiol* **571**, 461–476.

Rall W (1969). Time constants and electrotonic length of membrane cylinders and neurons. *Biophys J* **9**, 1483–1508.

Ramanathan S, Hanley JJ, Deniau JM & Bolam JP (2002). Synaptic convergence of motor and somatosensory cortical afferents onto GABAergic interneurons in the rat striatum. *J Neurosci* **22**, 8158–8169.

Sachdev RN, Ebner FF & Wilson CJ (2004). Effect of subthreshold up and down states on the whisker-evoked response in somatosensory cortex. *J Neurophysiol* **92**, 3511–3521.

Schubert D, Kotter R, Luhmann HJ & Staiger JF (2006). Morphology, electrophysiology and functional input connectivity of pyramidal neurons characterizes a genuine layer Va in the primary somatosensory cortex. *Cereb Cortex* **16**, 223–236.

Schubert D, Staiger JF, Cho N, Kotter R, Zilles K & Luhmann HJ (2001). Layer-specific intracolumnar and transcolumnar functional connectivity of layer V pyramidal cells in rat barrel cortex. *J Neurosci* **21**, 3580–3592.

Slaght SJ, Paz T, Chavez M, Deniau JM, Mahon S & Charpier S (2004). On the activity of the corticostriatal networks during spike-and-wave discharges in a genetic model of absence epilepsy. *J Neurosci* **24**, 6816–6825.

Smith Y, Raju DV, Pare JF & Sidibe M (2004). The thalamostriatal system: a highly specific network of the basal ganglia circuitry. *Trends Neurosci* **27**, 520–527.

Stern EA, Jaeger D & Wilson CJ (1998). Membrane potential synchrony of simultaneously recorded striatal spiny neurons *in vivo*. *Nature* **394**, 475–478.

Stern EA, Kincaid AE & Wilson CJ (1997). Spontaneous subthreshold membrane potential fluctuations and action potential variability of rat corticostriatal and striatal neurons in vivo. *J Neurophysiol* **77**, 1697–1715.

Strecker RE, Steinfels GF, Abercrombie ED & Jacobs BL (1985). Caudate unit activity in freely moving cats: effects of phasic auditory and visual stimuli. *Brain Res* **329**, 350–353.

Swadlow HA (2003). Fast-spike interneurons and feedforward inhibition in awake sensory neocortex. *Cereb Cortex* **13**, 25–32.

Wilent WB & Contreras D (2004). Synaptic responses to whisker deflections in rat barrel cortex as a function of cortical layer and stimulus intensity. *J Neurosci* **24**, 3985–3998.

Wilson CJ (1995*a*). The contribution of cortical neurons to the firing pattern of striatal spiny neurons. In *Models of Information Processing in the Basal Ganglia*, ed. Houk JC, Davies JL & Beiser DG, pp. 29–50. MIT Press, Cambridge, MA, USA.

Wilson CJ (1995*b*). Dynamic modification of dendritic cable properties and synaptic transmission by voltage-gated potassium channels. *J Comput Neurosci* **2**, 91–115.

Wilson CJ (2007). GABAergic inhibition in the neostriatum. *Prog Brain Res* **160**, 91–110.

Wilson CJ & Kawaguchi Y (1996). The origins of two-state spontaneous membrane potential fluctuations of neostriatal spiny neurons. *J Neurosci* **16**, 2397–2410.

Wilson JS, Hull CD & Buchwald NA (1983). Intracellular studies of the convergence of sensory input on caudate neurons of cat. *Brain Res* **270**, 197–208.

Wright AK, Norrie L, Ingham CA, Hutton EA & Arbuthnott GW (1999). Double anterograde tracing of outputs from adjacent "barrel columns" of rat somatosensory cortex. Neostriatal projection patterns and terminal ultrastructure. *Neuroscience* **88**, 119–133.

Wright AK, Ramanathan S & Arbuthnott GW (2001). Identification of the source of the bilateral projection system from cortex to somatosensory neostriatum and an exploration of its physiological actions. *Neuroscience* **103**, 87–96.

Zhu JJ & Connors BW (1999). Intrinsic firing patterns and whisker-evoked synaptic responses of neurons in the rat barrel cortex. *J Neurophysiol* **81**, 1171–1183.

Author contributions

S.C., M.P. and S.M. conceived the conceptual framework of the study and designed the experiments. M.P. and S.M. performed the experiments. M.P. performed the analysis and M.P., J.-M.D., S.M. and S.C. participated in the interpretation of the data. S.C. wrote the manuscript and M.P., J.-M.D. and S.M. revised and improved it. All the authors have approved the final version of the manuscript.

Acknowledgements

This work was supported by the Ministère Français de la Recherche, the Institut National de la Santé et de la Recherche Médicale and by grants from the Agence Nationale de la Recherche (ANR R06274DS, 2006) and the Programme Interdisciplinaire-CNRS Neuro IC 2010. We thank Anne-Marie Godeheu and Verena Aliane for histological processing.